New Journal of Physics
The open access journal at the forefront of physics

Deutsche Physikalische Gesellschaft DPG IOP Institute of Physics

PAPER • OPEN ACCESS

Polymerization of nitrogen in two theoretically predicted high-energy compounds ScN_6 and ScN_7 under modest pressure

To cite this article: Yanhui Guo *et al* 2022 *New J. Phys.* **24** 083015

New Journal of Physics
The open access journal at the forefront of physics

Deutsche Physikalische Gesellschaft DPG
IOP Institute of Physics

Published in partnership with: Deutsche Physikalische Gesellschaft and the Institute of Physics

OPEN ACCESS

RECEIVED
4 April 2022

REVISED
21 July 2022

ACCEPTED FOR PUBLICATION
26 July 2022

PUBLISHED
15 August 2022

PAPER

Polymerization of nitrogen in two theoretically predicted high-energy compounds ScN_6 and ScN_7 under modest pressure

Yanhui Guo, Shuli Wei*, Zhipeng Liu, Haiyang Sun, Guowei Yin, Shiju Chen, Ziyue Yu, Qiang Chang and Yuping Sun*

School of Physics and Optoelectronic Engineering, Shandong University of Technology, 250049, People's Republic of China
* Authors to whom any correspondence should be addressed.

E-mail: weishuli@sdut.edu.cn and sunyuping@sdut.edu.cn

Keywords: first-principles calculations, high pressure, high energy density

Abstract

Materials under high pressure usually exhibit unique chemical and physical properties. Polynitrogen compounds have received widespread attention as potential high energy density materials. This paper uses CALYPSO crystal structure prediction method to study the structures of ScN_6 and ScN_7 in 0–100 GPa. Theoretical calculations show that ScN_6 is thermodynamically stable above 80 GPa, while ScN_7 is thermodynamically stable from 30 GPa to 90 GPa. Furthermore, ScN_7 is metastable under ambient conditions, demonstrating that it can be quenched to ambient conditions after high pressure synthesis. The $P\bar{1}$-ScN_6 is a three-dimensional extended fold multi-nitrogen network, and the $P\bar{1}$-ScN_7 contains a five-membered ring and a curved N4 molecular unit. Both $P\bar{1}$-ScN_6 and $P\bar{1}$-ScN_7 contain a lot of N–N single bonds and N=N double bonds. The energy densities of $P\bar{1}$-ScN_6 and $P\bar{1}$-ScN_7 are 3.97 kJ g^{-1} and 3.12 kJ g^{-1}, respectively. The detonation velocity and detonation pressure of the $P\bar{1}$-ScN_6 phase and $P\bar{1}$-ScN_7 phase are also higher than that of TNT. Excellent energy storage properties and detonation performance show that they can be used as potential high-energy materials. These results opened up a new way for the synthesis of nitrogen-rich compounds.

1. Introduction

The content of nitrogen in the Earth's crust is very small. Most of the nitrogen in nature exists in the atmosphere in the form of elemental molecular nitrogen (about 78% of the air volume), which is bound by the strongest N≡N bond [1]. Because the energy difference of N–N bond (160 kJ mol^{-1}), N=N bond (418 kJ mol^{-1}) and N≡N bond (954 kJ mol^{-1}) is significant, molecules or ions containing nitrogen atoms will be released stably during decomposition a lot of energy, so nitrogen-containing molecules and ions are often used in fuels or explosives. The more nitrogen, the higher its energy density and detonation performance. Therefore, polynitrogen compounds have attracted extensive attention as potential high energy-density materials (HEDMs) [2, 3].

As an effective energy carrier, single-bonded nitrogen can only be obtained under high pressure and high temperature conditions due to its low dynamic stability [4]. In the past few decades, people have conducted a lot of exploration on nitrogen to find this kind of pure polymer nitrogen structure with high energy density [5, 6]. Until 2001 [7] and 2004 [8], Erements *et al* used laser-heated diamond anvil experimental methods to synthesize the single bond form of nitrogen cg-N for the first time under 240 GPa and 110 GPa/2000 K conditions, respectively. This nitrogen-containing polymer allotrope cg-N has a higher energy density, and the energy released during decomposition is five times that of HMX [9], but its synthesis pressure is higher and its stability is poor. Therefore, stabilizing this kind of nitrogen structures has become a current research hotspot.

At present, high pressure as a new method provides a lot of insights for the discovery of new materials, especially the exploration of high-density polynitrogen compounds [10]. High pressure can cause redistribution of electrons, change in conducting chemical bonds, and form more compounds with nitrogen atoms [11, 12]. Recent many research results have found that the addition of metal elements to pure nitrogen can induce the formation of new polynitrogen compounds under high pressure. For example, alkali metals (Li [13], Na [14, 15], K [16]), alkaline Earth metals (Be [17], Mg [18], Ca [19], Ba [20]) and transition metals (Fe [21], Cu [22, 23], Zn [24], Cd [25]). These nitrogen-containing compounds have a variety of configurations, such as isolated nitrogen atoms, a curved chain structure, ring structure, a three-dimensional extended network, those has a high degree of nitrogen polymerization, which is generally related to high energy density. To expand the scope of research on nitrogen-rich compounds, more and more researchers are focusing on transition metal polynitrogen compounds. In the study of Fe–N [21] system, the energy released when FeN_6 and FeN_8 decompose are 4.34 kJ g^{-1} and 4.70 kJ g^{-1}, respectively. And the energy density is almost close to energy released by the decomposition of TNT [26], even higher than TNT, and energy storage of transition metal polynitrogen compounds has begun to make breakthroughs. In addition, Zhu *et al* [19] conducted a theoretical study on the Ca–N compound at a pressure of 0–100 GPa and obtained several new forms of poly-nitrogen compounds. Based on the above research results, this paper carried out the prediction of the transition metal Sc–N system. In the same cycle, the transition metal element Sc has one more valence electron than the alkaline Earth metal element Ca, which plays a significant role in the formation of polynitrides. A lot of studies have been done on Sc–N compounds. As early as 2001 [27], Gagliardi *et al* predicted that the high-energy molecule ScN_7 containing $[\eta^7\text{-}N_7]^{3-}$ ligand might exist, but there is no clear crystal structure information. In three reports in 2018 [28] and 2021 [29, 30] the researchers predicted and proved the existence of Sc_4N_3, Sc_8N_7, ScN, ScN_3 and ScN_5 molecules under high pressure, but for the high nitrogen contents of ScN_6 and ScN_7 still have not been discovered. We expect to find this high-energy nitrogen search methods combined with DFT calculations to study ScN_6 and ScN_7. It is worth noting that we successfully predicted these two unknown high pressure phases: $P\bar{1}$-ScN_6 and $P\bar{1}$-ScN_7. The higher the degree of polymerization of the nitrogen compound will result in the greater the energy density. So, the research on rich-N Sc–N compound will help to obtain more polynitrogen configuration, then to discover novel potential HEDMs.

2. Methods

In this paper, we mainly search for stable ScN_x ($x = 6$–7) compounds in the moderate pressure range (within 100 GPa) [31–34], we implemented crystal structure searching method CALYPSO [35, 36] to predict the potential structure of ScN_6 and ScN_7 at 0, 40, 80 and 100 GPa, respectively. In order to find all stable crystal structures, one up to four formula units were used. Vienna *ab initio* simulation package (VASP) [37] was used for structural optimization and energy calculation and within the DFT framework. The PBE [38] as the exchange correlation functional under the generalized gradient approximation was adopted. Using the projected augmented wave [39] method of Sc and N potentials, $3d^14s^2$ and $2s^22p^3$ were calculated as the valence electrons of Sc and N atoms. The kinetic cut-off energy was 800 eV, and the Brillouin zone used a reciprocal space resolution of $2\pi \times 0.03$ Å to ensure that all enthalpy calculations converge well to 1 meV/atom. The images of the crystal structures were generated by the VESTA software [40]. The dynamic stability was judged by the phonon frequency, and the phonon frequency of all considered structures was calculated by PHONOPY code [41]. The charge calculation was based on Bader analysis [42]. The density of states (DOS) and electronic local function (ELF) [43, 44] were calculated by VASP code. Crystal orbital Hamilton population (COHP) [45] on Sc–N compounds was performed by using the LOBSTER [46] code to explain the bonding.

3. Results and discussions

In this study, the CALYPSO structure prediction method was used to search for the structures of Sc–N compounds under 0–100 GPa, and the convex hull diagram was constructed as shown in figure 1(a). The convex hull is a powerful way to judge the stability of special stoichiometric compounds under high pressure [47, 48]. According to the standard, only the structures located on the convex hull are the most stable, and the structures located above the convex hull are the metastable or unstable structure. Figure 1(a) shows the most favorable ScN_x structures obtained structural research method under different pressures. Solid Sc [49] and solid N [50] under different pressure are used as reference structures. The convex hull shows that ScN, ScN_3, ScN_5, ScN_6, ScN_7 are stable structures in different pressure ranges. Among them, compared with the results of previous studies [28], two new stoichiometry ScN_6 and ScN_7

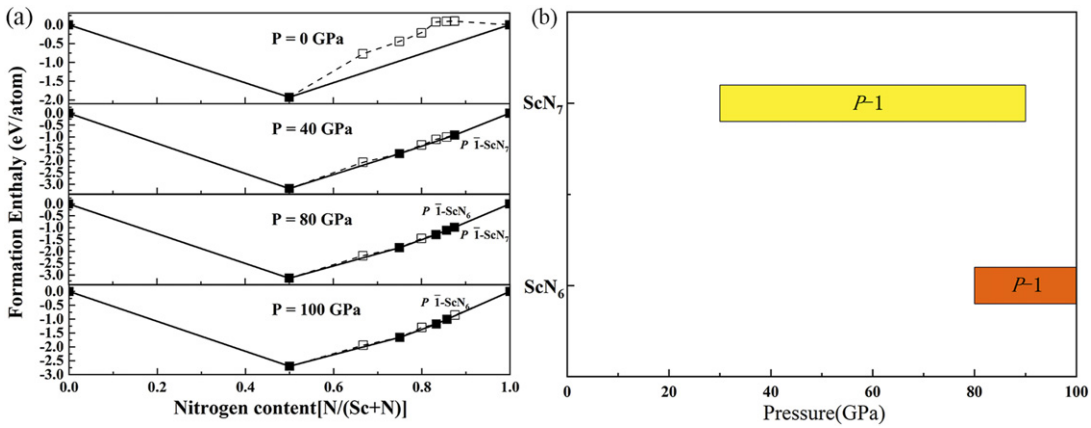

Figure 1. (a) Enthalpies of formation of various ScN_x ($x = 1$–7) compounds under pressure. (b) Calculated thermodynamically stable pressure ranges for ScN_6 and ScN_7 compounds.

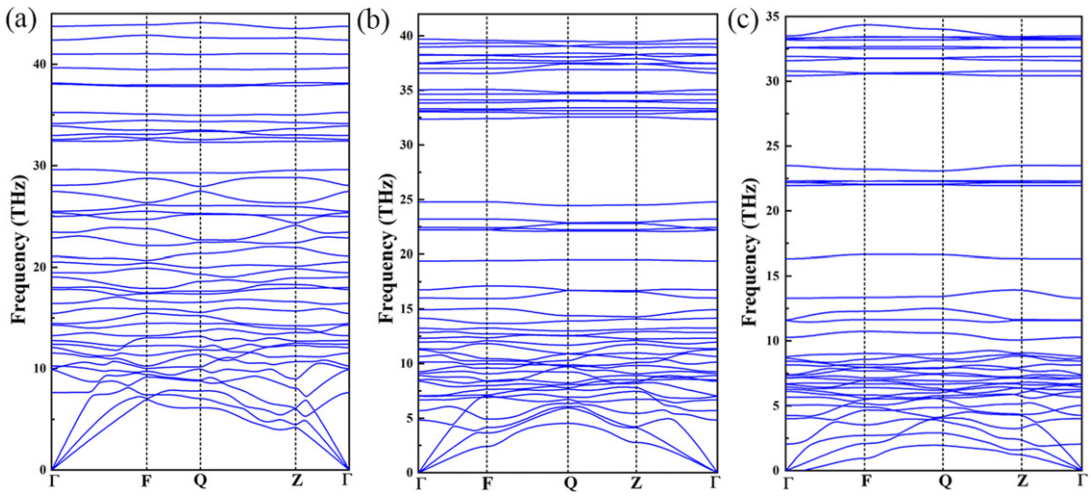

Figure 2. Phonon dispersion curves for $P\bar{1}$-ScN_6 at $P = 80$ GPa (a), $P\bar{1}$-ScN_7 at $P = 30$ GPa (b) and $P\bar{1}$-ScN_7 at $P = 0$ GPa (c).

were firstly found in this paper. The complete pressure composition phase diagram of ScN_6 and ScN_7 compound is shown in figure 1(b). The two compounds have no phase transition in the whole pressure range of 0–100 GPa and both have $P\bar{1}$ space group. As shown in figure 1(b), ScN_6 was stable in the 80–100 GPa range, and ScN_7 was stable in the 30–90 GPa pressure range. Besides, the phonon dispersion curves under high pressure and ambient conditions can prove their mechanical and kinetic stability, which is shown in figures 2(a)–(c), these structures not have imaginary frequencies. Which means that the $P\bar{1}$-ScN_7 is not only synthesized at moderate pressure, but also can be quenched to ambient conditions.

The crystal structures of ScN_6 and ScN_7 phases were predicted as shown in figures 3(a)–(d). The ScN_6 adopts monoclinic $P\bar{1}$ structure when $P = 80$ GPa, and the crystal structure diagram is shown in figure 3(a). The $P\bar{1}$-ScN_6 is a three-dimensional extended fold multi-nitrogen network structure that 26 nitrogen atoms form a large ring and interconnect to a polymerized nitrogen network, as shown in figure 3(c). At 80 GPa, the closest distance between N–N atoms in $P\bar{1}$-ScN_6 is 1.28 Å and the farthest distance is 1.47 Å, which is very close to the standard bond lengths of N=N double bonds (1.25 Å) and N–N single bonds (1.45 Å) [18], respectively. It shows that there are some single and double bonds in this $P\bar{1}$-ScN_6 structure. Besides, another high-pressure compound $P\bar{1}$-ScN_7 was predicted under modest pressure, and it is stable in the range of 30–90 GPa. The $P\bar{1}$-ScN_7 contains two nitrogen configurations: N5 five-membered ring and curved N4 molecular unit. This structure can be regarded as a sandwich structure consisting of alternating arrangements of Sc atoms, curved N4 units and N5 five-membered rings, as shown in figures 3(b) and (d). The shortest distance of N–N atoms of $P\bar{1}$-ScN_7 is 1.30 Å and the farthest distance is 1.32 Å, between the single N–N bonds and double N=N bonds, indicating that there are alternate N–N bonds and N=N bonds in the novel high-pressure structure. The corresponding crystal structure parameters and distances between N atoms are shown in tables 1 and 4.

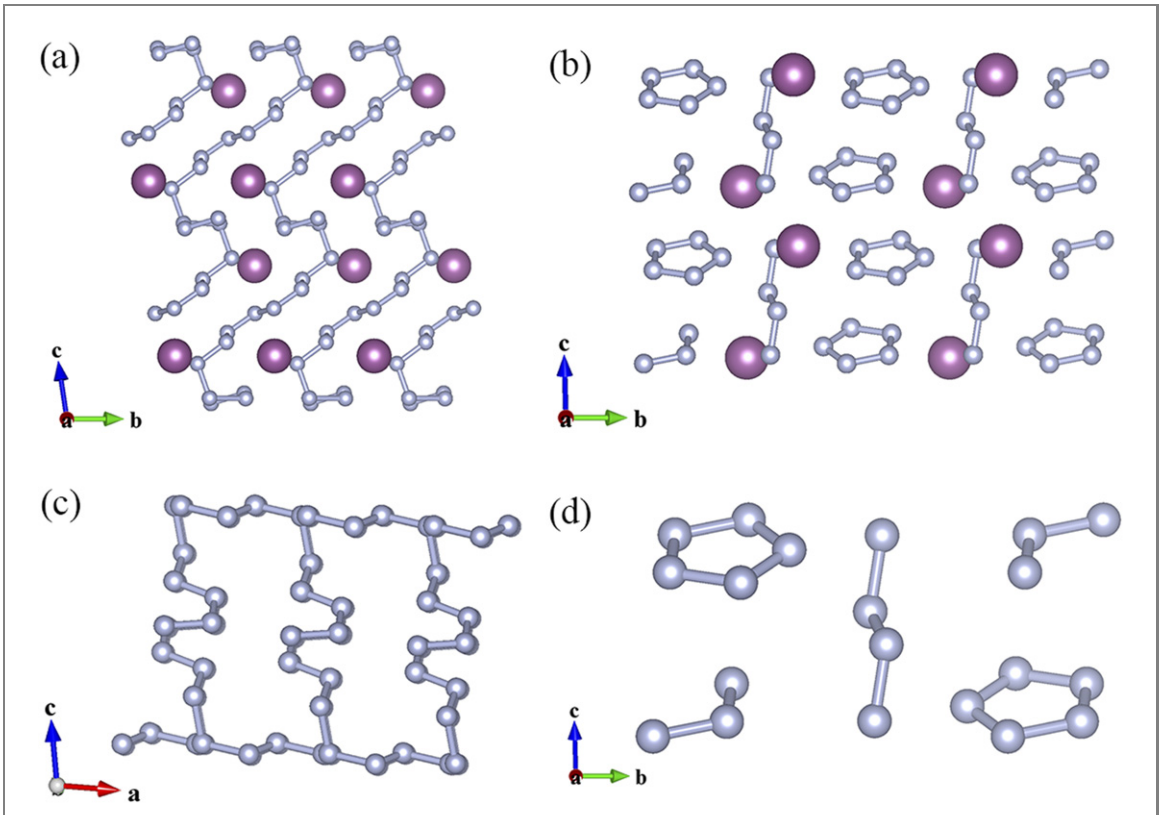

Figure 3. Structural views of $P\overline{1}$-ScN_6 at $P = 80$ GPa (a), $P\overline{1}$-ScN_7 at $P = 30$ GPa (b), 3D extended puckered poly-nitrogen network in $P\overline{1}$-ScN_6 (c) and N5 five-membered rings and N4 molecular unit in $P\overline{1}$-ScN_7 (d). The blue balls are nitrogen atoms, as well as purple balls are scandium atoms.

Table 1. Structural parameters of all considered structures for Sc–N.

Str. And S.G.	Lattice parameters (Å, °)	Atomic coordinates (fractional)	Sites
$P\overline{1}$-ScN_6, $P = 80$ GPa	$a = 3.701$, $\alpha = 95.69$, $b = 3.890$, $\beta = 97.68$, $c = 6.709$, $\gamma = 105.82$	N1 (0.475, 0.680, 0.999)	2i
		N2 (0.509, 0.750, 0.802)	2i
		N3 (0.416, 0.429, 0.679)	2i
		N4 (0.269, 0.595, 0.375)	2i
		N5 (0.688, 0.099, 0.515)	2i
		N6 (0.887, 0.326, 0.971)	2i
		Sc1 (0.940, 0.032, 0.242)	2i
$P\overline{1}$-ScN_7, $P = 30$ GPa	$a = 4.078$, $\alpha = 94.78$, $b = 6.349$, $\beta = 78.97$, $c = 5.228$, $\gamma = 107.22$	N1 (0.689, 0.065, 0.189)	2i
		N2 (0.340, 0.143, 0.861)	2i
		N3 (0.827, 0.116, 0.651)	2i
		N4 (0.341, 0.745, 0.240)	2i
		N5 (0.618, 0.918, 0.686)	2i
		N6 (0.664, 0.521, 0.445)	2i
		N7 (0.288, 0.518, 0.809)	2i
		Sc1 (0.152, 0.366, 0.174)	2i

Energy calculations show that the energy density of $P\overline{1}$-ScN_6 released by the decomposition to ScN and N_2 is as high as 3.97 kJ g^{-1}, which is greater than that of the same main group transition metal nitrides, such as zinc nitride (ZnN_6 is 2.72 kJ g^{-1}) [24], and close to that of iron nitride (FeN_6 is 4.34 kJ g^{-1}) [21]. Besides, the energy density of $P\overline{1}$-ScN_7 is 3.12 kJ g^{-1}, higher than that of LiN_5 (2.72 kJ g^{-1}) [13] and modern highenergy materials such as TATB and RDX, which usually have energy densities ranging from 1 to 3 kJ g^{-1} [51]. The detonation velocity and detonation pressure are the most important factors determining its detonation performance. And the detonation velocity and detonation pressure of the ScN_x ($x = 6, 7$) structure are estimated by the Kamlet–Jacobs empirical equations [52] are compared with those of TNT and HMX explosives [53]. As show in table 2, the detonation velocity and detonation pressure of the $P\overline{1}$-ScN_6 phase are estimated to be as high as 13.04 km s^{-1} and 98.68 GPa, which are nearly 2 and 5 times that of TNT, while the detonation velocity and detonation pressure of the $P\overline{1}$-ScN_7 phase are 9.83 km s^{-1} and 48.04 GPa, nearly 1.5 and 2 times that of TNT. The detonation performance of the two is

Table 2. Comparison of the detonation velocity and detonation pressure of ScN_x ($x = 6, 7$) structures estimated using Kamlet–Jacobs empirical equations [52] with the TNT and HMX explosives [53].

Compounds	ρ (g cm^{-3})	E_g (kJ g^{-1})	E_v (kJ cm^{-3})	D (km s^{-1})	P (GPa)
$P\bar{1}$-ScN_6	3.13	3.97	12.42	13.04	98.68
$P\bar{1}$-ScN_7	2.23	3.12	6.96	9.83	48.04
TNT	1.64	4.30	7.05	6.90	19
HMX	1.90	5.70	10.83	9.10	39.3

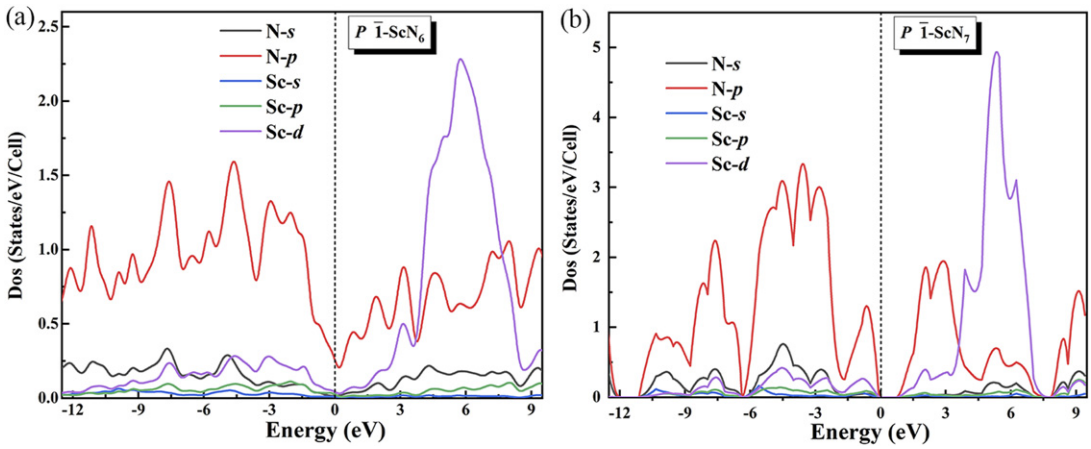

Figure 4. Calculated projected DOS for (a) $P\bar{1}$-ScN_6 at $P = 80$ GPa, (b) $P\bar{1}$-ScN_7 at $P = 30$ GPa.

Table 3. Calculated Bader charges for $P\bar{1}$-ScN_6 and $P\bar{1}$-ScN_7, respectively.

Str. And S.G.	Atom	N	Charge value (e)	δ (e)
$P\bar{1}$-ScN_6	N1	2	5.11	0.11
	N2	2	5.38	0.38
	N3	2	5.25	0.25
	N4	2	5.19	0.19
	N5	2	5.27	0.27
	N6	2	5.38	0.38
	Sc	2	1.42	−1.58
$P\bar{1}$-ScN_7	N1	2	5.21	0.21
	N2	2	5.12	0.12
	N3	2	5.09	0.09
	N4	2	5.17	0.17
	N5	2	5.12	0.12
	N6	2	5.24	0.24
	N7	2	5.73	0.73
	Sc	2	1.32	−1.68

much higher than that of TNT, so both of these two high-pressure Sc–N compounds can be used as potential high-energy-density materials.

From figure 4, the electronic structure DOS analysis shows that $P\bar{1}$-ScN_6 is metallic, and the N-2p state contributes the most near the Fermi level. The $P\bar{1}$-ScN_7 is estimated to be a semiconductor with a band gap of 1.25 eV (we calculated the band gap of $P\bar{1}$-ScN_7 is 2.19 eV by using the more accurate HSE06), the vicinity of the Fermi energy level is mainly contributed by N-2p orbitals. The main reason for this is that the metal element Sc transferring part of the charges to N when the metal element is introduced. In order to better understand the effect of N-2p orbitals on the electronic properties of the compound, we have analyzed the values of charge transfer. According to the Bader charge analysis, for $P\bar{1}$-ScN_6, each Sc atom transfers 1.58e to the N atom. And for $P\bar{1}$-ScN_7, each Sc atom transfers 1.68e to the N atom. The corresponding charge transfer values are shown in table 3. Based on the above analysis, the Sc atom acts as an electron donor to provide electrons to the N atom.

In order to analyze their bonding form, we analyzed the ELF. The $P\bar{1}$-ScN_6 is a three-dimensional extended fold multi-nitrogen network, the nitrogen atom adopts two hybrid forms of sp^2 and sp^3. As shown

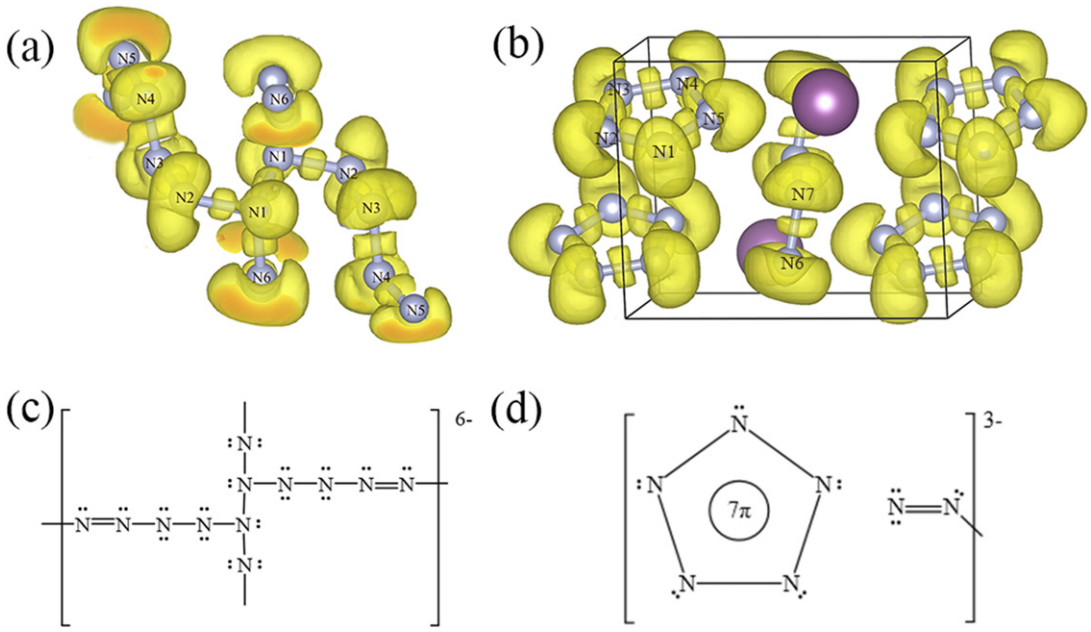

Figure 5. The 3D ELF of polymeric nitrogen configurations in $P\bar{1}$-ScN_6 (a) and $P\bar{1}$-ScN_7 (b), respectively, Lewis structures of polynitrogen forms in $P\bar{1}$-ScN_6 (c) and $P\bar{1}$-ScN_7 (d), respectively.

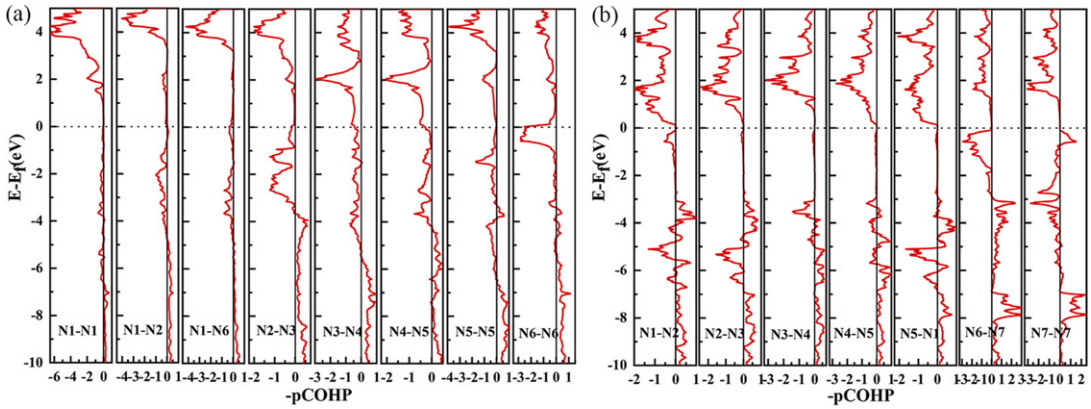

Figure 6. Calculated pCOHP for all N–N pairs in (a) $P\bar{1}$-ScN_6 and (b) $P\bar{1}$-ScN_7 compound. Negative values represent anti-bonding states, zero means non-bonding state, and positive values represent bonding states.

in figures 5(a) and (c), only the N1 atom and the adjacent N atom form three N–N σ bonds through three sp^3 hybrid orbitals, and the remaining sp^3 hybrid orbitals are filled with electrons to form a lone pair of electron pairs. For each N2, N3, and N6 atom, there are one σ bonds with adjacent N atoms on each side, and two sp^3 hybrid orbitals participate in the bonding. There are two remaining sp^3 hybrid orbitals are not participate in bonding, so they are filled to form lone pairs. For each N4 and N5 atom, the nitrogen atoms are in sp^2 hybridization forms, there are two sp^2 hybrid orbitals involved in bonding, one side has a σ bond and a π bond with the adjacent N atom to form a N=N bond, and the remaining side has a σ bond with the adjacent N atom. The remaining sp^2 hybrid orbitals do not participate in bonding, so they are filled to form lone pairs. For $P\bar{1}$-ScN_7, there are two polynitrogen forms: ring N5 unit and N4 molecular unit, as shown in figure 5(b). Through the ELF distribution of electrons, it is found that the hybridization form of all nitrogen atoms is sp^2. For the N5 ring molecular plane, the two sp^2 hybrid orbitals of each N atom and the sp^2 hybrid orbitals of adjacent N atoms form two σ bonds on both sides, and the remaining sp^2 hybrid orbitals are filled with electrons to form a single lone electron pair. Out-of-plane, seven delocalized π electrons form a set of aromatic π bonds, resulting in the alternation of single and double bonds in the N5 ring. Similar to the ring N5 unit, for the nitrogen atom in the N4 molecular unit, each nitrogen atom at both ends has an N=N bond, which consists of a σ bond occupying a sp^2 hybrid orbital and a π bond. The remaining two sp^2 hybrid orbital is filled with electrons, forming two lone electrons pairs. In addition to an N=N bond, each nitrogen atom in the middle also hybridizes with the sp^2 orbital of the other end atom to

Table 4. Calculated integrated crystal orbital Hamiltonian populations of N–N pairs without inclusion of spin polarization in $P\bar{1}$-ScN_6 and $P\bar{1}$-ScN_7.

Str. And S.G.	Atom	Atom	Distance (Å)	ICOHP (E_f)	Str. And S.G.	Atom	Atom	Distance (Å)	ICOHP (E_f)
$P\bar{1}$-ScN_6, $P = 80$ GPa	N1	N1		−5.20	$P\bar{1}$-ScN_7, $P = 30$ GPa	N1	N2		−9.16
	N 2s	N 2s	1.47	0.100		N 2s	N 2s	1.30	1.13
	N 2s	N 2p		−1.22		N 2s	N 2p		−3.75
	N 2p	N 2p		−4.08		N 2p	N 2p		−6.54
	N1	N2		−6.90		N2	N3		−8.92
	N 2s	N 2s	1.39	0.93		N 2s	N 2s	1.31	1.13
	N 2s	N 2p		−3.19		N 2s	N 2p		−3.61
	N 2p	N 2p		−4.64		N 2p	N 2p		−6.44
	N1	N6		−7.39		N3	N4		−9.06
	N 2s	N 2s	1.38	0.82		N 2s	N 2s	1.30	1.28
	N 2s	N 2p		−3.26		N 2s	N 2p		−3.81
	N 2p	N 2p		−4.95		N 2p	N 2p		−6.53
	N2	N3		−7.11		N4	N5		−9.43
	N 2s	N 2s	1.35	0.59		N 2s	N 2s	1.30	1.32
	N 2s	N 2p		−2.64		N 2s	N 2p		−3.98
	N 2p	N 2p		−5.06		N 2p	N 2p		−6.77
	N3	N4		−8.78		N5	N1		−8.81
	N 2s	N 2s	1.29	0.41		N 2s	N 2s	1.33	1.14
	N 2s	N 2p		−2.33		N 2s	N 2p		−3.64
	N 2p	N 2p		−6.86		N 2p	N 2p		−6.31
	N4	N5		−9.23		N6	N7		−8.63
	N 2s	N 2s	1.29	1.04		N 2s	N 2s	1.32	0.82
	N 2s	N 2p		−4.09		N 2s	N 2p		−3.63
	N 2p	N 2p		−6.18		N 2p	N 2p		−5.82
	N5	N5		−7.08		N7	N7		−8.20
	N 2s	N 2s	1.37	0.33		N 2s	N 2s	1.31	0.63
	N 2s	N 2p		−2.09		N 2s	N 2p		−2.54
	N 2p	N 2p		−5.32		N 2p	N 2p		−6.29
	N6	N6		−6.64					
	N 2s	N 2s	1.37	0.50					
	N 2s	N 2p		−2.28					
	N 2p	N 2p		−4.86					

form a σ bond. The remaining one sp^2 hybrid orbital is filled with electrons, forming one lone electron pair. The corresponding Lewis structure is shown in figure 5(d). By analyzing the ELF of the above structure, it can be concluded that both $P\bar{1}$-ScN_6 and $P\bar{1}$-ScN_7 contain a lot of N–N single bonds and N=N double bonds, especially the N atoms of $P\bar{1}$-ScN_6, have a relatively high degree of polymerization, therefore they all have a high energy density.

The pCOHP can divide the bond energy into bond energy and anti-bond energy, and shows the overlap strength. The positive value corresponds to the bonding states, and the negative value corresponds to the anti-bonding states. Figure 6(a) shows that for $P\bar{1}$-ScN_6, it can be seen that the Fermi level is located in the anti-bonding states. Since the bonded states and the anti-bonded states correspond to fully occupied and partially unoccupied orbitals, respectively, the cross of the anti-bonded region implies electronic instability near the Fermi energy level, which is consistent with the metal properties in the DOS analysis. The bonding states of $P\bar{1}$-ScN_6 is fully occupied, while the anti-bonding states is not fully occupied. Therefore, a covalent bond can be formed between adjacent nitrogen atoms. The bond strength between the orbitals in the $P\bar{1}$-ScN_6 compound can be expressed by the theoretical value of ICOHP in table 4. For $P\bar{1}$-ScN_6, the values of ICOHP between N1–N1, N1–N2, N1–N6, N2–N3, N3–N4, N4–N5, N5–N5 and N6–N6 pairs are −5.20, −6.90, −7.39, −7.11, −8.78, −9.23, −7.08, −6.64, respectively. This means covalent bond formation, these results indicate that the interaction of N4–N5 is stronger than that of other pairs. This also consistent with the previous analysis of N4 and N5 forming N=N double bonds. Figure 6(b) shows that for $P\bar{1}$-ScN_7, the Fermi level is located in the non-bonding state, which is consistent with the semiconductor properties in DOS analysis. Similar to $P\bar{1}$-ScN_6, the bonding states of $P\bar{1}$-ScN_7 is fully occupied, while the anti-bonding states is not fully occupied. Therefore, a covalent bond can also be formed between adjacent nitrogen atoms. The theoretical values of ICOHP is also used to express the bonding strength between the

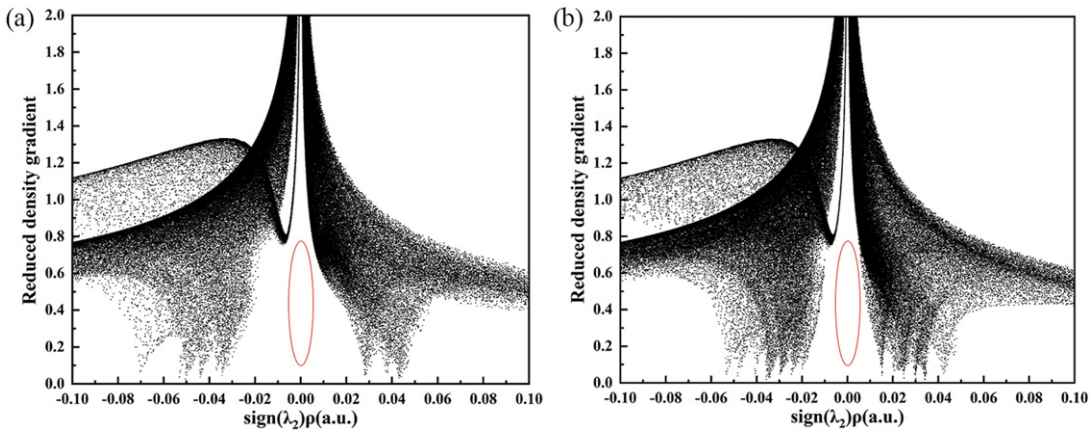

Figure 7. Plots of RDG versus electron density multiplied by the sign of the second Hessian eigenvalue for $P\bar{1}$-ScN_6 (a), $P\bar{1}$-ScN_7 (b).

orbitals in the $P\bar{1}$-ScN_7 compound. For $P\bar{1}$-ScN_7, the values of ICOHP between N1–N2, N2–N3, N3–N4, N4–N5, N5–N1, N6–N7 and N7–N7 pairs are −9.16, −8.92, −9.06, −9.43, −8.81, −8.63, −8.20, respectively. The results show that the interactions between the N1–N1, N2–N3, N3–N4, N4–N5, N5–N1 and N6–N7 pairs are stronger than the N7–N7 pairs. This also corresponds to the previous analysis of N6–N7 forming a double bond and N7–N7 forming a single bond.

Since noncovalent interactions not be determined by ELF calculations, a reduced density gradient (RDG) is introduced for identification, further judgment is made by passing the sign (sign(λ_2)) of the second largest eigenvalue of the electron density Hessian matrix. RDG is defined as $s = (2(3\pi^2))^{-1}|\nabla \rho|\rho^{-4/3}$. To distinguish between different types of interactions, we multiply the RDG by the sign of the second Hessian eigenvalue of $\nabla 2\rho$ (sign(λ_2)) [54, 55]. The corresponding 2D RDG results are shown in figure 7. The abscissa eigenvalues (sign(λ_2)ρ(a.u.)) can be defined as three corresponding intervals. The red area in the figure 7 is the interaction of vdW. The left side shows strong and attractive weak interactions which the most common ones that conform to this feature are hydrogen bonds, including strong halogen bonds. The right side corresponds to the strong steric effect region that appears in the ring and cage. Noncovalent interactions are marked by one or more spikes in regions of low density, low gradients. It is evident from the figure 7 that the values of sign(λ_2)ρ(a.u.) are 0.044 and 0.042 for ScN_6 and ScN_7, respectively, indicating the presence of non-bonding overlap, this is typical of cyclic species such as benzene [54–56]. So there are rings in both high-pressure structures. This also corresponds to the structure of the two compounds.

4. Conclusions

In this paper, the first-principles calculation combined with CALYPSO crystal structure prediction method was used to search the structures of Sc–N system at 0–100 GPa. We successfully predicted two unknown high pressure phases: $P\bar{1}$-ScN_6 and $P\bar{1}$-ScN_7, and the $P\bar{1}$-ScN_6 is thermodynamically stable above 80 GPa, the $P\bar{1}$-ScN_7 is thermodynamically stable in the pressure range of 30 GPa to 90 GPa. In addition, ScN_7 is metastable under ambient conditions, indicating that it can be quenched to ambient conditions after high pressure synthesis. The DOS analysis shows that $P\bar{1}$-ScN_6 is metallic and the $P\bar{1}$-ScN_7 is a semiconductor and the Fermi energy level is mainly contributed by the N-2p orbital. The $P\bar{1}$-ScN_6 is a three-dimensional extended fold multi-nitrogen network, and the nitrogen atom adopts two hybrid forms of sp^2 and sp^3. The $P\bar{1}$-ScN_7 contains a five-membered ring and a curved N4 molecular unit, and the nitrogen atom adopts one hybrid forms of sp^2. Both $P\bar{1}$-ScN_6 and $P\bar{1}$-ScN_7 contain a lot of N–N single bonds and N=N double bonds, and the energy calculation shows that the energy density released by decomposition of $P\bar{1}$-ScN_6 is as high as 3.97 kJ g^{-1}, and that of $P\bar{1}$-ScN_7 is 3.12 kJ g^{-1}, which is higher than that of modern high energy materials. The detonation velocity and detonation pressure of the $P\bar{1}$-ScN_6 phase are estimated to be nearly 2 and 5 times that of TNT, respectively, while for $P\bar{1}$-ScN_7 phase, the detonation velocity and detonation pressure are also higher than that of TNT. Excellent energy storage properties and detonation performance show that the two high-pressure $P\bar{1}$-ScN_6 and $P\bar{1}$-ScN_7 structures can be used as a kind of potential high-energy material. This study can provide new insights into the understanding of polynitrides and encourages future experimental exploration of these promising materials.

Acknowledgments

This work was supported by the National Natural Science Foundation of China (No. 12104259), the Natural Science Foundation of Shandong Province (Nos. ZR2020QA059, ZR2019MA020), Open Project of State Key Laboratory of Superhard Materials, Jilin University (No. 202104), Shandong University of Technology PhD Funding.

Data availability statement

All data that support the findings of this study are included within the article (and any supplementary files).

ORCID iDs

Shuli Wei https://orcid.org/0000-0001-9554-1990
Yuping Sun https://orcid.org/0000-0002-1330-0155

References

[1] van der Ham C J M, Koper M T M and Hetterscheid D G H 2014 *Chem. Soc. Rev.* **43** 5183–91
[2] Singh R P, Verma R D, Meshri D T and Shreeve J M 2006 *Angew. Chem., Int. Ed.* **45** 3584–601
[3] Sun W, Holder A, Orvañanos B, Arca E, Zakutayev A, Lany S and Ceder G 2017 *Chem. Mater.* **29** 6936–46
[4] Tomasino D, Kim M, Smith J and Yoo C-S 2014 *Phys. Rev. Lett.* **113** 205502
[5] Goncharov A F, Gregoryanz E, Mao H-k, Liu Z and Hemley R J 2000 *Phys. Rev. Lett.* **85** 1262
[6] Mattson W D, Sanchez-Portal D, Chiesa S and Martin R M 2004 *Phys. Rev. Lett.* **93** 125501
[7] Mikhail E, Russell H, Hokwang M and Eugene G 2001 *Nature* **411** 170–4
[8] Eremets M I, Gavriliuk A G, Trojan I A, Dzivenko D A and Boehler R 2004 *Nat. Mater.* **3** 558–63
[9] Lin H, Zhu Q, Huang C, Yang D-D, Lou N, Zhu S-G and Li H-Z 2019 *Struct. Chem.* **30** 2401–8
[10] Zhang L, Wang Y, Lv J and Ma Y 2017 *Nat. Rev. Mater.* **2** 17005
[11] Wang X, Li J, Xu N, Zhu H, Hu Z and Chen L 2015 *Sci. Rep.* **5** 16677
[12] Zhu H, Zhang F, Ji C, Hou D, Wu J, Hannon T and Ma Y 2013 *J. Appl. Phys.* **113** 033511
[13] Peng F, Yao Y, Liu H and Ma Y 2015 *J. Phys. Chem. Lett.* **6** 2363–6
[14] Popov M 2005 *Phys. Lett.* A **334** 317–25
[15] Steele B A and Oleynik I I 2016 *Chem. Phys. Lett.* **643** 21–6
[16] Ji C, Zhang F, Hou D, Zhu H, Wu J, Chyu M-C, Levitas V I and Ma Y 2011 *J. Phys. Chem. Solids* **72** 736–9
[17] Wei S, Li D, Liu Z, Wang W, Tian F, Bao K, Duan D, Liu B and Cui T 2017 *J. Phys. Chem.* C **121** 9766–72
[18] Yu S, Huang B, Zeng Q, Oganov A R, Zhang L and Frapper G 2017 *J. Phys. Chem.* C **121** 11037–46
[19] Zhu S, Peng F, Liu H, Majumdar A, Gao T and Yao Y 2016 *Inorg. Chem.* **55** 7550–5
[20] Huang B and Frapper G 2018 *Chem. Mater.* **30** 7623–36
[21] Jiao F, Zhang C and Xie W 2020 *J. Phys. Chem.* C **124** 19953–61
[22] Yi W, Zhao K, Wang Z, Yang B, Liu Z and Liu X 2020 *ACS Omega* **5** 6221–7
[23] Li J, Sun L, Wang X, Zhu H and Miao M 2018 *J. Phys. Chem.* C **122** 22339–44
[24] Shi X, Yao Z and Liu B 2020 *J. Phys. Chem.* C **124** 4044–9
[25] Niu S, Li Z, Li H, Shi X, Yao Z and Liu B 2021 *Inorg. Chem.* **60** 6772–81
[26] Hang G-y, Yu W-l, Wang T and Wang J-t 2019 *Comput. Mater. Sci.* **156** 77–83
[27] Gagliardi L and Pyykkö P 2001 *J. Am. Chem. Soc.* **123** 9700–1
[28] Aslam M A and Ding Z J 2018 *ACS Omega* **3** 11477–85
[29] Lin J, Peng D, Wang Q, Li J, Zhu H and Wang X 2021 *Phys. Chem. Chem. Phys.* **23** 6863–70
[30] Wei S, Liu Z, Guo Y, Sun H, Chang Q and Sun Y 2021 *J. Phys.: Condens. Matter* **33** 475401
[31] Liu Z, Li D, Tian F, Duan D, Li H and Cui T 2020 *Inorg. Chem.* **59** 8002–12
[32] Pourovskii L V 2019 *J. Phys.: Condens. Matter* **31** 373001
[33] Zhang Z *et al* 2021 *Phys. Rev. Lett.* **128** 047001
[34] Xie H *et al* 2020 *J. Phys. Chem. Lett.* **11** 646–51
[35] Wang Y, Lv J, Zhu L and Ma Y 2010 *Phys. Rev.* B **82** 094116
[36] Wang Y, Lv J, Zhu L and Ma Y 2012 *Comput. Phys. Commun.* **183** 2063–70
[37] Kresse G and Furthmüller J 1996 *Comput. Mater. Sci.* **6** 15–50
[38] Perdew J P, Burke K and Ernzerhof M 1996 *Phys. Rev. Lett.* **77** 18
[39] Kresse G and Furthmüller J 1996 *Phys. Rev.* B **54** 16
[40] Momma K and Izumi F 2011 *J. Appl. Cryst.* **44** 1272–6
[41] Togo A, Oba F and Tanaka I 2008 *Phys. Rev.* B **78** 134106
[42] Tang W, Sanville E and Henkelman G 2009 *J. Phys.: Condens. Matter* **21** 084204
[43] Savin A, Nesper R, Wengert S and Fässler T F 1997 *Angew. Chem.* **109** 1892–918
[44] Steinmann S N, Mo Y and Corminboeuf C 2011 *Phys. Chem. Chem. Phys.* **13** 20584–92
[45] Deringer V L, Tchougréeff A L and Dronskowski R 2011 *J. Phys. Chem.* A **115** 5461–6
[46] Maintz S, Deringer V L, Tchougréeff A L and Dronskowski R 2016 *J. Comput. Chem.* **37** 1030–5
[47] Peng F, Botana J, Wang Y, Ma Y and Miao M 2016 *J. Phys. Chem. Lett.* **7** 4562–7
[48] Feng J, Hennig R G, Ashcroft N W and Hoffmann R 2008 *Nature* **451** 445–8
[49] Ormeci A, Koepernik K and Rosner H 2006 *Phys. Rev.* B **74** 104119
[50] Pickard C J and Needs R J 2009 *Phys. Rev. Lett.* **102** 125702

[51] Evans W J, Lipp M J, Yoo C-S, Cynn H, Herberg J L, Maxwell R S and Nicol M F 2006 *Chem. Mater.* **18** 2520–31
[52] Kamlet M J and Jacobs S J 1968 *J. Chem. Phys.* **48** 23–35
[53] Zhang J, Oganov A R, Li X and Niu H 2017 *Phys. Rev.* B **95** 020103
[54] Johnson E R, Keinan S, Mori-Sánchez P, Contreras-García J, Cohen A J and Yang W 2010 *J. Am. Chem. Soc.* **132** 6498–506
[55] Otero-de-la-Roza A, Johnson E R and Luaña V 2014 *Comput. Phys. Commun.* **185** 1007–18
[56] Yuan J, Xia K, Wu J and Sun J 2020 *Sci. China Phys. Mech. Astron.* **64** 218211